

# Electrochemical Immunosensors for Detection of Cancer Protein Biomarkers

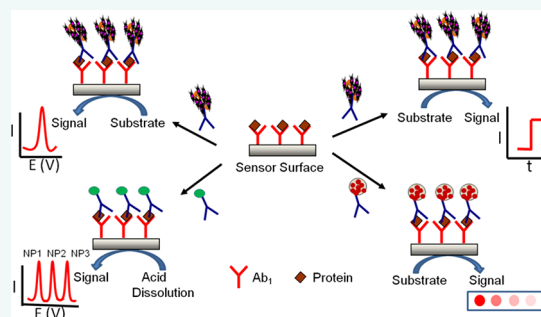
Bhaskara V. Chikkaveeraiah,<sup>†,‡</sup> Ashwinkumar A. Bhirde,<sup>‡</sup> Nicole Y. Morgan,<sup>†</sup> Henry S. Eden,<sup>§</sup> and Xiaoyuan Chen<sup>‡,\*</sup>

<sup>†</sup>Microfabrication and Microfluidics Unit, Biomedical Engineering and Physical Science Shared Resource, <sup>‡</sup>Laboratory of Molecular Imaging and Nanomedicine (LOMIN), National Institute of Biomedical Imaging and Bioengineering (NIBIB), and <sup>§</sup>Intramural Research Program, NIBIB, National Institutes of Health, Bethesda, Maryland 20892, United States

A biomarker is defined as “a characteristic that is objectively measured and evaluated as an indicator of normal biological processes, pathogenic processes, or pharmacological responses to a therapeutic intervention”.<sup>1</sup> One important class of biomarkers includes proteins that, when present at elevated or depressed concentrations in serum, tissue, or saliva, can be indicative of disease states. The development of reliable, cost-effective, powerful detection and monitoring strategies for cancer is particularly important, due to the disease's prevalence, high rates of recurrence, and potential lethality. To avoid false positives in cancer diagnosis that can arise from population variations in expression of a single biomarker, simultaneous measurements of a panel of protein biomarkers are typically required.<sup>2–4</sup> These biomarker panels hold enormous potential for early cancer detection and personalized therapy.<sup>5–7</sup>

This review focuses on the development of electrochemical detection strategies for cancer protein biomarkers, including prostate-specific antigen (PSA), prostate-specific membrane antigen (PSMA), platelet factor 4 (PF-4), interleukin 6 (IL-6), interleukin 8 (IL-8), carcinoembryonic antigen (CEA), cancer antigens (e.g., CA-125, CA-199), c-reactive protein (CRP), and  $\alpha$ -feto-protein (AFP). As an example, PSA is produced by the cells of the prostate gland and is typically elevated in the presence of prostate cancer. The threshold level in clinical screening is 4 ng mL<sup>-1</sup>, with normal PSA levels in healthy men generally lower and PSA levels in cancer patients usually found in a range from the threshold up to 10 ng mL<sup>-1</sup>.<sup>8</sup> Prostate-specific membrane antigen is a cell surface glycoprotein expressed by prostate epithelial cells and found at elevated levels in patients with prostate

## ABSTRACT



Bioanalytical methods have experienced unprecedented growth in recent years, driven in large part by the need for faster, more sensitive, more portable (“point of care”) systems to detect protein biomarkers for clinical diagnosis. Electrochemical detection strategies, used in conjunction with immunosensors, offer advantages because they are fast, simple, and low cost. Recent developments in electrochemical immunosensors have significantly improved the sensitivity needed to detect low concentrations of biomarkers present in early stages of cancer. Moreover, the coupling of electrochemical devices with nanomaterials, such as gold nanoparticles, carbon nanotubes, magnetic particles, and quantum dots, offers multiplexing capability for simultaneous measurements of multiple cancer biomarkers. This review will discuss recent advances in the development of electrochemical immunosensors for the next generation of cancer diagnostics, with an emphasis on opportunities for further improvement in cancer diagnostics and treatment monitoring. Details will be given for strategies to increase sensitivity through multilabel amplification, coupled with high densities of capture molecules on sensor surfaces. Such sensors are capable of detecting a wide range of protein quantities, from nanogram to femtogram (depending on the protein biomarkers of interest), in a single sample.

**KEYWORDS:** biomarkers · electrochemistry · immunoassay · amplification · microfluidics · nanomaterials · multiplexing

cancer. Abnormal levels of PSMA are also associated with solid tumors such as breast, lung, ovary, bladder, and intestinal tract cancers.<sup>9,10</sup> Interleukin-6 is a multifunctional cytokine associated with several different cancers, including head and neck squamous cell carcinoma (HNSCC). Mean serum IL-6 levels in healthy individuals are typically less

\* Address correspondence to shawn.chen@nih.gov.

Received for review May 30, 2012 and accepted July 26, 2012.

Published online July 27, 2012  
10.1021/nn3023969

This article not subject to U.S. Copyright. Published 2012 by the American Chemical Society

than  $6 \text{ pg mL}^{-1}$ , whereas in patients with HNSCC, the levels are  $20 \text{ pg mL}^{-1}$  or greater.<sup>11</sup> Serum IL-6 is also elevated in colorectal, gastrointestinal, and prostate cancers. Carcinoembryonic antigen is a glycoprotein most often associated with colorectal cancer but also found at elevated levels in patients with breast cancer, ovarian cancer, and lung cancer. The normal levels of CEA in healthy adults are in the range of  $3\text{--}5 \text{ ng mL}^{-1}$ , although these levels increase up to  $10 \text{ ng mL}^{-1}$  in some benign diseases.<sup>12</sup> The broad range of clinically relevant concentrations for different biomarkers presents challenges for multiplexed detection. At the same time, the large variations in biomarker levels among healthy individuals suggest that accurate diagnosis will require measurement of a panel of biomarkers rather than a single test.

Today, most clinical protein biomarker detection is done using an enzyme-linked immunosorbent assay (ELISA),<sup>13</sup> but requirements for relatively expensive test kits and bulky plate readers limit ELISA's usefulness for point of care (POC) diagnostics. LC-MS-based proteomics are gaining importance for biomarker discovery but are currently too expensive and technically complex for routine clinical diagnostics.<sup>14,15</sup> Alternatively, antibody-coated microarrays are being developed in 96- or 384-well plate format using colorimetric detection methods (Quansys Biosciences, SABiosciences). These arrays are simple and highly selective and allow multiplexed measurement of proteins.<sup>16–19</sup> At present, there are several commercially available automated or semiautomated analyzers for multiplexed protein measurements, employing fluorescence (Luminex, Myriad RBM), electrochemiluminescence (ECL) (Roche Diagnostics, Mesoscale Discovery), or surface plasmon resonance (Horiba Inc., BIO-RAD) measurement technologies. Assay kits are available for measurement of up to 10 selected target proteins per sample with detection limits (DL) of  $1\text{--}100 \text{ pg mL}^{-1}$  in serum.<sup>4</sup> These commercial instruments require specialized consumables, including sample well plates, chips, and reagent kits<sup>20</sup> which are expensive and, thus, limit their usefulness for point of care applications where resources are limited. Fluorescence-based detection strategies typically require laser sources and precise alignment of optical components, whereas electrochemical detection strategies offer robust, quantitative measurements using low-cost, simple instrumentation.<sup>21,22</sup>

Devices for POC detection of protein biomarkers must be sensitive, robust, simple to operate, and low cost. For successful clinical application, they must also be accurate for normal as well as elevated levels of target protein concentrations and be resistant to interference from nontargeted proteins. Such systems could enable rapid and inexpensive cancer testing in decentralized and under-resourced settings. New technologies using nanomaterials—such as magnetic particles, gold nanoparticles, quantum dots, and

**VOCABULARY:** **biomarker** - a biomolecule whose presence or level of expression is indicative of the presence or severity of some disease state; **immunoassay** - a way of measuring biomolecule concentration in biological liquids, such as human serum, by means of antibody–antigen interaction; **amplification** - an increase in the magnitude or strength of signal, such as electric current, or light intensity to reach a lower detection limit; **multiplexing** - in the context of this paper, detecting multiple biomarkers in a biological liquid of interest to increase the confidence level of disease prediction; **electrode** - a conductive substrate on which the entire protein biomarker detection scaffold is assembled

carbon nanotubes—are being developed to increase the sensitivity of electrochemical detection of cancer biomarkers.<sup>23</sup> The low detection limits achievable by such methods could facilitate early detection of cancer and offer greater diagnostic accuracy. This review focuses on different strategies for electrochemical detection of protein biomarkers, especially those applicable to POC testing for cancer. The review begins with a brief overview of different electrochemical methods in use for immunosensor development. Then there are sections that discuss immunosensors based on magnetic beads, the use of multienzyme labels, and immunoassays using nanoparticles as labels. Next, the use of carbon nanotubes for improved electrode performance is discussed in detail followed by sections on electrochemiluminescence and recent advances in coupling electrochemical immunosensors with microfluidics. The final section covers recent demonstrations of electrochemical measurements by paper-based microfluidic devices. Although these devices have not yet been employed for cancer biomarker detection, paper-based microfluidics show tremendous promise for bringing down the cost per assay.

**Electrochemical Methods.** Various forms of voltammetry (linear sweep, differential pulse, square-wave, stripping) and amperometry are the most widely used electrochemical methods for detection of protein biomarkers. These methods work as follows: (1) a tracer antibody is labeled with an electroactive species, such as an enzyme, metal nanoparticle, or quantum dot; (2) the tracer is allowed to bind with analyte, possibly through an intermediate primary antibody, and thus immobilized on an electrode surface; and (3) the concentration of the targeted biomarker is quantified by applying a potential and measuring the resulting current at the electrode. In essence, the applied potential drives a redox reaction of the labeled electroactive species and provides a current signal that is proportional to the concentration of the antibody-bound analytes. The various versions of voltammetry differ in the waveform of the applied voltage and the phase of the waveform during which currents are measured. Stripping voltammetry (SV) is a special case

in which the electroactive species are ionic species and is typically used for the determination of trace amounts of metals in solution. The applied potential necessary for oxidation (stripping) of the metal ions can be used to discriminate among multiple metal species, allowing nearly simultaneous measurement of different analytes. For biomarkers, this type of multiplexed measurement can be achieved by attaching different metal or nanoparticle tags to the respective secondary antibodies.

Electrochemical detection strategies employing nanostructured surfaces, nanoparticle labels, and magnetic beads offer new opportunities for highly sensitive protein detection.<sup>4,24–27</sup> Most of the strategies discussed below employ the sandwich immunoassay approach, in which the sensor surface is first functionalized with capture antibodies ( $Ab_1$ ) or aptamers to capture the protein analyte of interest. After the introduction of the sample, and rinsing steps, a tracer enzyme- or nanoparticle-labeled antibody ( $Ab_2$ ) is added to bind to the captured analyte protein. The use of multiply labeled antibodies or other amplification strategies (e.g., enzyme-labeled magnetic beads or gold nanoparticles) can enhance the sensitivity of the detection. A summary of the assorted measurement strategies, the achieved limits of detection, and the linear range of detection for different biomarkers can be found in Table 1.

**Magnetic-Bead-Based Immunoassays.** The use of magnetic beads to develop diagnostic devices is gaining in popularity. For example, magnetic beads have been used as substrates for the capture antibodies or for target antigens in immunoassays and enzyme-linked immunoassays.<sup>21,28–32</sup> Magnetic beads have fast reaction kinetics compared to bulk solid surfaces, high surface area per unit volume (owing to their small diameter), and good stability.<sup>33,34</sup> Moreover, the relative ease of surface modification with functional groups, DNA, enzymes, or antibodies greatly contributes to the utility of beads in development of sensitive, rapid electrochemical immunoassay systems.<sup>35,36</sup>

Figure 1 shows a typical immunoassay scheme in which magnetic beads are used for solution-based capture of analytes and then drawn to the surface using an external magnet for electrochemical detection. Zani *et al.* employed this scheme in 8-electrode, screen-printed array format for the detection of PSA.<sup>37</sup> PSA was captured on the magnetic beads, and the captured beads were bathed with AP-enzyme-labeled antibody and measured using differential pulse voltammetry, achieving a detection limit of  $1.4 \text{ ng mL}^{-1}$  for the PSA.

Sarkar *et al.* reported electrochemical detection of free PSA (f-PSA) using magnetic beads on a 3-electrode screen-printed sensor.<sup>38</sup> They performed immunoassays on the magnetic beads in a cuvette with horseradish peroxidase (HRP)-labeled secondary antibodies,

then transferred the beads to the sensor surface. Upon introduction of the hydrogen peroxide substrate, Sarkar *et al.* used the amperometric response of the HRP labels to measure the analyte concentrations on the beads, with a detection limit (DL) of  $<0.1 \text{ ng mL}^{-1}$  f-PSA. Wang and co-workers reported an ultrasensitive sandwich immunoassay for immunoglobulin G (IgG) that used anti-IgG-modified magnetic beads to capture IgG, followed by the addition of polystyrene tags functionalized with DNA and anti-IgG.<sup>39</sup> After binding, the DNA was released from the tags in alkaline solution, dipurinated by acid, and measured by stripping potentiometry of the free guanine nucleobases at the graphite electrode, achieving a DL of  $2 \text{ pg mL}^{-1}$ . Using a similar immunoassay protocol, Munge *et al.* used square-wave voltammetry, a substrate of 1-naphthyl phosphate, and carbon nanotube (CNT) tags conjugated with thousands of catalytic alkaline phosphatase (AP) enzymes for signal amplification to achieve an ultralow detection of  $67 \text{ aM}$  of IgG.<sup>40</sup> Willner and Katz demonstrated another strategy employing magnetic beads to control the bioelectrocatalytic processes that can be employed for developing immunosensors.<sup>22</sup> Rotation of magnetic particles (MPs) by external magnetic fields, to increase bioelectrocatalytic activity, is a common practice, and Willner and Katz studied the effect of such rotation on the kinetics of electron transfer in two bioelectrocatalytic systems (pyrroloquinoline-quinone-functionalized MPs that oxidize NADH, and ferrocene-functionalized MPs that mediate the bioelectrocatalyzed oxidation of glucose in the presence of glucose oxidase).<sup>41</sup>

**Multienzyme-Labeled Immunoassays.** Signal amplification for target protein detection can be achieved by loading greater numbers of biomolecules or multienzymes onto nanoparticle probes. Magnetic beads, CNTs, polymer beads, and streptavidin–biotin complexes have been used for multienzyme labeling to achieve signal amplification. A major factor affecting the sensitivity of the detection strategy is the nonspecific binding (NSB) of bioconjugates (enzyme-labeled  $Ab_2$ ) that arises when the bioconjugates bind to non-antigen sites on the sensor during immunoassay fabrication. In NSB, the bioconjugates generate a signal, but it is not proportional to the analyte concentration, which can raise the detection limit of the strategy and decrease the sensitivity of the assay. NSB can be minimized by washing with bovine serum albumin or casein with a small quantity of detergent such as Tween-20 in the wash buffer in NSB blocking steps in the assay. There is no universal blocking agent for NSB in any type of protein detection system. To avoid NSB arising from a potential amplification strategy, a thorough characterization of the amplifying formulation is needed. An NSB blocking protocol for any specific assay is often a trial and error process. Wang *et al.* reported the use of multienzyme-labeled CNTs for

**TABLE 1. Protein Detection Limits Using Different Electrochemical Methods Described in This Paper**

strategy	biomarkers	sample volume, $\mu\text{L}$	labels	detection limit	linear range	ref
stripping voltammetry	IgG	35	AuNPs	3 pM	0.5–100 ng/mL	52
	cardiotroponin I	50	Ag	0.5 ng/mL	0.8–5 ng/mL	53
	$\beta$ -microglobulin g	50	ZnS		N/A	54
	IgG		CdS	3.3 fmol		
	BSA		PbS	7.5 fmol		
square-wave voltammetry	CRP		CuS			
	IgG	50	SWCNT-AP	67 aM	50–150 fg/mL	40
differential pulse voltammetry	IgG	50	polystyrene-DNA	2 pg/mL	0.1–500 ng/mL	39
	PSA	950	Ab <sub>2</sub> -AP	1.4 ng/mL	0–20 ng/mL	37
amperometry	T-PSA	NA	label free	0.25 ng/mL	NA	67
	hlgG	150	AuNP-HRP	260 pg/mL	NA	49
	PSA	10	MB-HRP	0.5 pg/mL	0–10 pg/mL	43
	fPSA	20	Ab <sub>2</sub> -HRP	<0.1 ng/mL	0–1 ng/mL	38
	IL-6	10	biotin-Ab <sub>2</sub> -Str-HRP	10 pg/mL	20–4000 pg/mL	46
	MMP-3	10	polybead-HRP	4 pg/mL	4–300 pg/mL	47
	IL-8	10	Str-MB-HRP	1 fg/mL	1–500 fg/mL	44
	CEA	NA	MB-Au-HRP	10 pg/mL	0.01–160 ng/mL	45
			GHS-HRP	1.5 pg/mL	0.01–200 ng/mL	48
		IL-6	10	MWCNT-HRP-Ab <sub>2</sub>	0.5 pg/mL	0.5–5 pg/mL
cyclic voltammetry amperometry	IL-6 & PSA	5	MWCNT-HRP-Ab <sub>2</sub>	8 pg/mL	8–1000 pg/mL	51
	PSA	10	MWCNT-HRP-Ab <sub>2</sub>	5 pg/mL	5–4000 pg/mL	
	PSA	10	MWCNT-HRP-Ab <sub>2</sub>	4 pg/mL	0.4–40 ng/mL	42
	AFP	NA	label free	8 pg/mL	0.25–250 ng/mL	65
	IL8 mRNA & IL-8 & IL-1 $\beta$			10 aM	0–10 pM	96
	IL-8 & IL-1 $\beta$	4		200 fg/mL	NA	
	IL-8 mRNA & IL-8	50	antifluorescein-HRP	3.9 fM	5 fM–50 pM	97
	IL-8		HRP-Ab <sub>2</sub>	7.4 pg/mL	10–500 pg/mL	
	CEA & CA 15-3 & PSA	NA	HRP-Ab <sub>2</sub>	0.2 ng/mL	0–200 ng/mL	98
	PSA & IL-6	5	MB-HRP-Ab <sub>2</sub>	5.2 U/mL	0–80 U/mL	
electrochemiluminescence	PSA			2 ng/mL	0–80 ng/mL	
	PSA & IL-6			0.23 pg/mL	0–20 pg/mL	99
	IL-6	1	Ab <sub>2</sub> -Poly-HRP	0.3 pg/mL	0–20 pg/mL	
	CEA	100	CdTe Qdots	10 fg/mL	10–1300 fg/mL	100
	TNF- $\alpha$	100		0.01 ng/mL	0.05–200 ng/mL	73
	PSA	20	thiocoline- [Ru(bpy) <sub>3</sub> ] <sup>2+</sup>	3.4 pg/mL	NA	75
	A-fetoprotein	5	AuNR-GOx-Ab <sub>2</sub>	8 pg/mL	0.01–8 ng/mL	76
	PSA	225	Ab <sub>2</sub> -AuNP-DNA-hemin	1 fg/mL	0.01 pg/mL–1 ng/mL	77
	p-53	50	[Ru(bpy) <sub>3</sub> ] <sup>2+</sup> -NHS	1.7 pg/mL	NA	80
	CRP	20	Ab <sub>2</sub> -[Ru(bpy) <sub>3</sub> ] <sup>2+</sup>	10 pg/mL	0.01–1000 ng/mL	81
	CRP	20	MB-PSB- [Ru(bpy) <sub>3</sub> ] <sup>2+</sup>	10 ng/mL	0.01–10 $\mu\text{g/mL}$	83
	CRP	50	liposome- [Ru(bpy) <sub>3</sub> ] <sup>2+</sup>	100 ng/mL	0.1–10 $\mu\text{g/mL}$	84
	AFP	50	Ab <sub>2</sub> -[Ru(bpy) <sub>3</sub> ] <sup>2+</sup>	5 pg/mL	0.5–8000 ng/mL	82
	PSA	10	Ab <sub>2</sub> -Si-[Ru(bpy) <sub>3</sub> ] <sup>2+</sup>	40 pg/mL	0.04–5 ng/mL	85
	PSA & IL-6	5	Ab <sub>2</sub> -Si-[Ru(bpy) <sub>3</sub> ] <sup>2+</sup>	1 pg/mL	0.001–10 ng/mL	86
CEA	NA	Au-SiO <sub>2</sub> -CdSe-CdS	0.25 pg/mL	0.0025–2 ng/mL		
AFP & CA-125 & CA 199 & CEA	2	Ab <sub>2</sub> -[Ru(bpy) <sub>3</sub> ] <sup>2+</sup>	64 fg/mL	0.32 pg/mL–10 ng/mL	88	
			0.15 ng/mL	0.5–100 ng/mL	94	
			0.6 U/mL	1.0–100 U/mL		
			0.17 U/mL	0.5–100 U/mL		
			0.5 ng/mL	1.0–100 ng/mL		

ultrasensitive detection of DNA and protein (IgG).<sup>21</sup> Multiwalled carbon nanotubes (MWCNTs) were coated with detection antibodies and thousands of alkaline phosphatase enzymes, resulting in detection of proteins at the femtomolar level. In subsequent work, they used a layer-by-layer (LbL) approach in conjunction with square-wave voltammetry to achieve a DL of

67 aM for IgG in buffer.<sup>40</sup> In the LBL method, MWCNTs (which are negatively charged) were coated with four alternating layers of poly(diallyl dimethyl ammonium chloride) (PDDA), which is cationic, and alkaline phosphatase (AP), which is anionic. Finally, these multiple layers were given a coating of PDDA, then poly(sodium-4-styrenesulfonate) (PSS) and anti-IgG

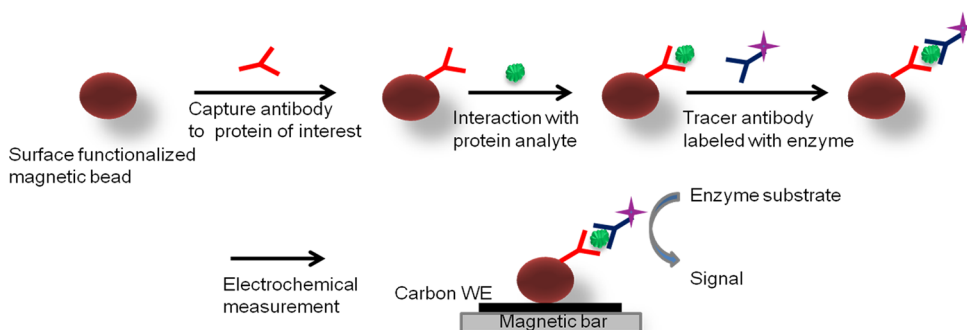


**Figure 1.** Scheme of the sandwich assay for protein biomarker detection using magnetic beads. Antibody-modified magnetic beads capture the protein from sample solution, followed by binding of a second enzyme-labeled antibody. Enzyme's substrate is used to develop the electrochemical signal. WE is the working electrode.

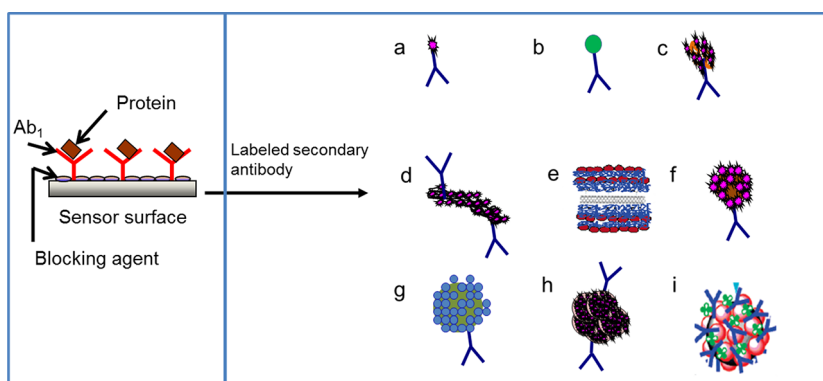


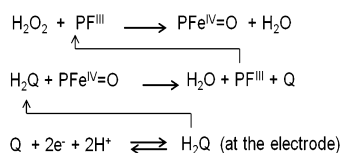
**Figure 2.** Bioconjugates for signal amplification strategies in electrochemical immunosensors. After the capture antibody is immobilized on the sensor surface, and the analyte protein is captured, these bioconjugates bind with analyte in a sandwich immunoassay. An electrochemical signal is generated using a substrate suitable for the electroactive species (typically an enzyme) on the bioconjugate probe. (a)  $Ab_2$ -enzyme, (b)  $Ab_2$ -nanoparticle, (c)  $Ab_2$ -biotin-streptavidin-enzyme, (d)  $Ab_2$ -CNT-enzyme,<sup>42</sup> (e) CNT-(PDDA-AP)<sub>4</sub>-PDDA-PSS tag,<sup>40</sup> (f) multienzyme- $Ab_2$ -nanoparticle,<sup>43</sup> (g)  $Ab_2$ -nanoparticle-Qdots, (h)  $Ab_2$ -MB-multienzyme clusters,<sup>44</sup> (i) MB-AuNP- $Ab_2$ -multienzyme.<sup>45</sup>

antibody. The LBL result was the bioconjugate MWCNT-(PDDA/AP)<sub>4</sub>-PDDA-PSS- $Ab_2$  (Figure 2e). To run the assay, magnetic beads that had been coated with  $Ab_1$  were used to capture IgG, after which the MWCNT bioconjugates were allowed to bind to the IgG. The catalytic product of AP with 1-naphthyl phosphate was detected using a CNT-modified glassy carbon electrode. The LBL approach yielded a 10-fold increase in the detection limit for the target DNA. Careful attention is required when MWCNTs are used for bioconjugation during the separation of unbound biomolecules. Usually, the mixture is centrifuged and supernatant (unbound biomolecules) is removed to separate the conjugated MWCNTs. Multiple washings of the bioconjugates are essential to remove the unbound entities completely to avoid the free unbound biomolecules in the bioconjugate dispersion which affect the sensitivity of detection strategy.

Rusling *et al.* fabricated a gold nanoparticle (AuNP) immunosensor by depositing a dense, 5 nm layer of glutathione-decorated AuNPs onto a 0.5 nm polycation layer, atop a pyrolytic graphite surface.<sup>43</sup> A DL of 0.5  $\mu\text{g mL}^{-1}$  for PSA was achieved using 1  $\mu\text{m}$  magnetic-bead- $Ab_2$ -HRP bioconjugates, coated with

$\sim 7500$  HRPs per bead (Figure 2f), and the PSA in patient samples was successfully measured with good correlation to commercial ELISA results. Immunosensor responses were measured by rotating disk amperometry, using  $\text{H}_2\text{O}_2$  substrate to activate  $\text{HRPFe}^{\text{III}}$  to a ferryl-oxoHRP species ( $\text{HRPFe}^{\text{IV}}=\text{O}$ ) and hydroquinone ( $\text{H}_2\text{Q}$ ) as a mediator for the reduction of  $\text{HRPFe}^{\text{IV}}=\text{O}$  (Scheme 1), which resulted in a steady state current proportional to protein concentration. Separation of the magnetic bead bioconjugates from unbound  $Ab_2$  and HRP is easy compared to other multienzyme bioconjugates. A simple external magnet can be used to isolate the conjugated magnetic beads from the suspension. Rusling *et al.* also reported a AuNP immunosensor that used  $Ab_2$ -biotin-streptavidin-enzyme bioconjugates (Figure 2c), instead of labeled magnetic beads, to achieve a DL of 10  $\mu\text{g mL}^{-1}$  for IL-6 in calf serum.<sup>46</sup> The accuracy of this AuNP immunosensor was demonstrated by determining IL-8 in conditioned growth media from HNSCC cells, which gave good correlation to results from a commercial ELISA kit.<sup>44</sup> In another strategy, 0.5  $\mu\text{m}$  multilabeled polymeric beads (polybeads-HRP- $Ab_2$ ) were used to achieve a DL of 10  $\mu\text{g mL}^{-1}$  for matrix metalloproteinase 3 (MMP-3) in calf serum.<sup>47</sup>

An amplification strategy using thionine-doped magnetic gold nanospheres multiply labeled with HRP (Figure 2i) has been reported, capable of detecting CEA at 5 pg mL<sup>-1</sup>.<sup>45</sup> In this work, a sandwich immunoassay was built on an anti-CEA/protein-A/gold nanoparticle-modified carbon fiber microelectrode and the electrochemical signal was developed by the reduction of H<sub>2</sub>O<sub>2</sub> by HRP labels on the magnetic gold nanospheres. The same sandwich assay, assembled directly on gold electrodes rather than carbon fiber electrodes, was used for the detection of CEA with a DL of 10 pg mL<sup>-1</sup>.<sup>48</sup> Ambrosi *et al.* reported a magnetic microbead-based immunoassay that used gold nano-



**Scheme 1.** Protein detection chemistry employing amperometry using HRP (PFe<sup>III</sup>) labels. Iron heme enzyme (PFe<sup>III</sup>) is oxidized to ferryl oxy species upon reaction with H<sub>2</sub>O<sub>2</sub> and then is reduced by the mediator hydroquinone (H<sub>2</sub>Q), resulting in the formation of water and quinone (Q). Quinone gets reduced at the electrode back to hydroquinone, giving rise to an electrical signal.

particles labeled with anti-human IgG, HRP-conjugated antibody to enhance the signal and obtained a detection limit of 260 pg mL<sup>-1</sup> for human IgG.<sup>49</sup> Carbon nanotubes have also been very successfully used as substrates for multiple enzyme labels. Malhotra *et al.* demonstrated an ultrasensitive electrochemical immunosensor used to measure a broad concentration range of the oral cancer biomarker IL-6 in a representative panel of HNSCC cells.<sup>50</sup> The immunosensor used a carbon nanotube forest electrode, together with MWCNTs with multiple labeling (Figure 4b). When using MWCNTs decorated with Ab<sub>2</sub> and 106 (average) HRP labels per nanotube (Figure 2d), a detection limit of 0.5 pg mL<sup>-1</sup> was obtained, as compared with a DL of 30 pg mL<sup>-1</sup> obtained when using streptavidin bound to biotinylated Ab<sub>2</sub> with 14–16 HRP (Figure 2c). Wan *et al.* also used MWCNTs multiply labeled with HRP and conjugated to secondary antibodies.<sup>51</sup> In conjunction with screen-printed carbon electrodes, they achieved multiplexed detection of PSA with a DL of 5 pg mL<sup>-1</sup> and IL-6 with a DL of 8 pg mL<sup>-1</sup> in buffer (Figure 3c).

**Nanoparticle-Labeled Immunoassays.** Nanoparticles exhibit physical or chemical properties that are different than the bulk form of the same materials.

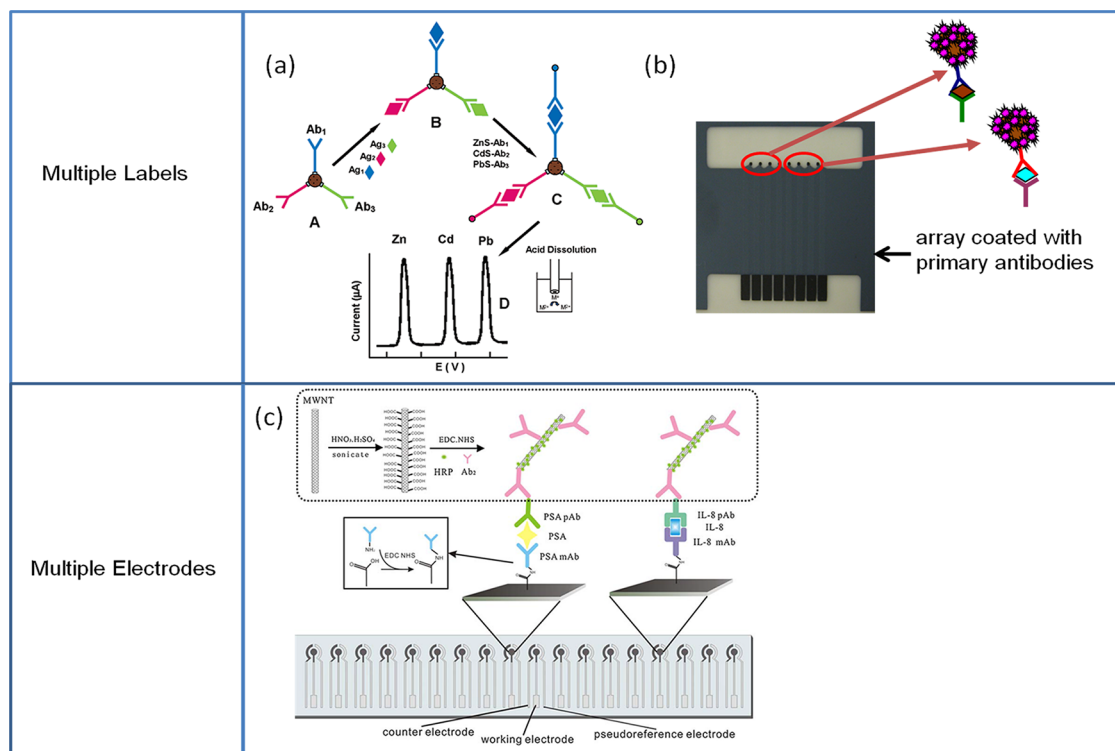


**Figure 3.** Multiprotein detection protocols using multiple labels or multiple electrodes. (a) Magnetic beads coated with differing primary antibodies are used to capture their corresponding antigens. Then, secondary antibodies labeled with differing inorganic nanocrystal tracers bind to the corresponding antigens. Following acid dissolution of the nanocrystals, the resulting ions are detected by electrochemical stripping. Adapted from ref 54. Copyright 2004 American Chemical Society. (b) Magnetic beads labeled with multienzymes and Ab<sub>2</sub> were used to capture specific analytes offline, and a sandwich immunoassay was performed on an 8-electrode array modified with different antibodies. (c) Multiplexed immunoassay using an array of screen-printed carbon electrodes modified with different capture antibodies employing universal MWCNT bioconjugates. Adapted with permission from ref 51. Copyright 2011 Elsevier.

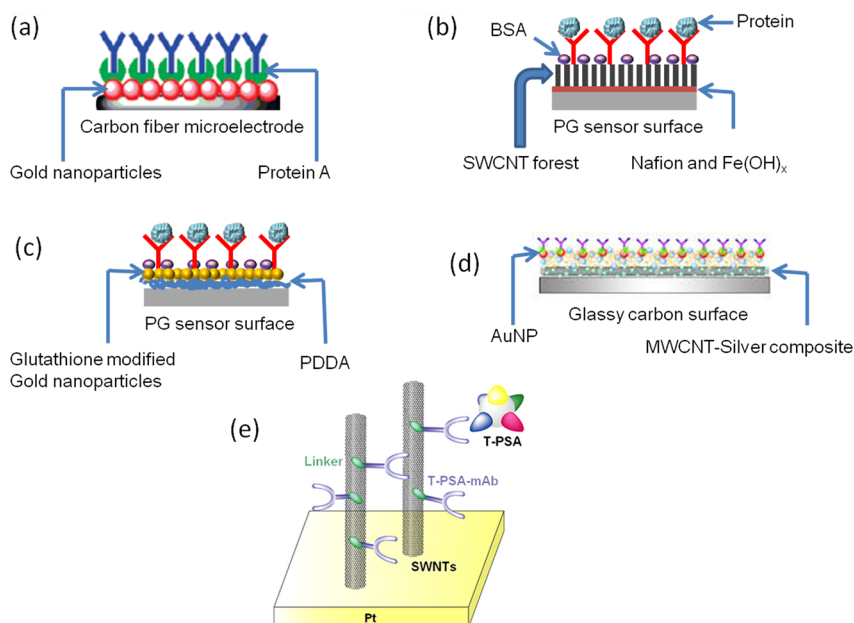


**Figure 4.** Different sensor surfaces for sandwich immunoassays, usable with electrochemical detection. (a) Carbon fiber microelectrode, modified with AuNP and protein A to capture a high density of primary antibodies. Adapted from ref 45. Copyright 2008 American Chemical Society. (b) SWCNT forest assembly developed on a pyrolytic graphite (PG) surface. Adapted from ref 50. Copyright 2010 American Chemical Society. (c) AuNP-modified pyrolytic graphite surface using layer-by-layer (LBL) approach. Adapted from ref 43. Copyright 2009 American Chemical Society. (d) Glassy carbon electrode modified with silver-MWCNT composite. Adapted with permission from ref 65. Copyright 2010 Elsevier. (e) SWCNT-modified Pt substrate used for label-free detection. Adapted with permission from ref 67. Copyright 2007 Elsevier.

Nanoparticles have larger surface area-to-volume ratios than macroparticles, which confers a higher binding efficiency in biomedical applications. Dequaire *et al.* first demonstrated the use of nanoparticles as direct labels in electrochemical immunoassays.<sup>52</sup> After  $Ab_2$ -nanoparticle bioconjugates bound to captured analytes, the nanoparticles were dissolved in acid to produce a large number of electroactive metal ions. The researchers obtained a DL of 3 pM for IgG in buffer, using anodic stripping voltammetry to measure the released gold ions. A strategy involving magnetic accumulation of gold nanoparticles, and their use to catalyze precipitation of Ag to produce large concentrations of electrochemically detectable metal ions, provided a DL of 0.5 ng mL<sup>-1</sup> for cardiac troponin I.<sup>53</sup> Liu *et al.* demonstrated an electrochemical immunoassay for simultaneous measurement of multiple proteins, involving multiple types of semiconductor nanocrystal labels (Figure 3a).<sup>54</sup> Anti- $\beta_2$ -microglobulin, anti-IgG, anti-bovine serum albumin, and anti-C-reactive protein antibodies were labeled with zinc sulfide, cadmium sulfide, lead sulfide, and copper sulfide nanocrystals, respectively, then allowed to bind with their target proteins on magnetic beads. The four species of metal ions, generated by dissolving the nanocrystals in acid, were separately detected using stripping voltammetry to achieve femtomole detection limits. Wang reviewed different strategies for conjugating  $Ab_2$ -nanoparticles or  $Ab_2$ -polymer beads with electroactive labels and releasing these labels for

electrochemical detection.<sup>55</sup> Daniels *et al.* reviewed immunosensors that use a label-free impedance method; this method usually requires additional amplification strategies to improve the sensitivity of detection.<sup>56</sup> Another interesting nanoparticle-based amplification strategy uses metal nanoparticle labels to catalyze subsequent silver deposition, bridging a gap between electrodes and leading to a readily measurable change in conductivity.<sup>57,58</sup> Park *et al.* used this method with AuNPs functionalized with oligonucleotides and gold electrodes functionalized with the complementary target DNA sequence, obtaining a detection limit of 500 fM target DNA.<sup>57</sup>

**Carbon-Nanotube-Based Electrode Surfaces.** Large surface area, high conductivity, and easy chemical modification are the highly desirable properties of electrode surfaces for use in electrochemical immunosensors. Carbon nanotubes are particularly well-suited for use in sensor surface modifications, due to their high chemical and thermal stability, large surface area per volume, and high conductivity.<sup>59</sup> The application of CNTs to electronic and electrochemical detection of biomolecules is very well reviewed, but we will briefly cover the most relevant developments here.<sup>60-62</sup> In most cases, nanotubes need to be functionalized before use. Treatment with strong acids, such as HNO<sub>3</sub> and H<sub>2</sub>SO<sub>4</sub>, imparts carboxyl groups, which can then be used for conjugation with biomolecules, such as proteins. Rusling's group developed nanostructured electrodes composed of densely packed films of

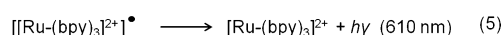
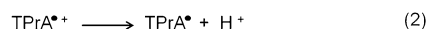
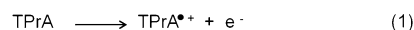
upright single-walled carbon nanotube (SWCNT) sections (forests) and used them for ultrasensitive detection of PSA.<sup>42</sup> The sensitivity of detection was further enhanced by attaching the tracer antibody to carbon nanotubes with multiple HRP labels giving a DL of 4 pg mL<sup>-1</sup> for PSA spiked into undiluted calf serum. A similar strategy was employed in a 4-electrode SWCNT forest array for simultaneous detection of multiple protein biomarkers in patient serum samples: PSA, prostate specific membrane antigen (PSMA), platelet factor 4 (PF-4), and IL-6.<sup>63</sup> The accuracy of the immunosensor was confirmed by cross validation with the corresponding ELISAs. SWCNT forests provided significant enhancement to the sensitivity of the immunosensor, due to a 10–15-fold greater number of capture antibodies immobilized on the sensor surface than on a flat immunosensor.<sup>64</sup> These results suggest that multiply labeled detection probes used in conjunction with electrode surfaces modified to yield a high capture density can result in immunosensor assemblies capable of detecting a wide range of protein concentrations with subpicogram per milliliter sensitivity. A comparison of immunosensors under similar assay conditions from Rusling's group revealed that the AuNP-modified platform yielded a 3-fold better detection limit than SWCNT-based immunosensors for the detection of IL-6 cancer biomarker in calf serum employing Ab<sub>2</sub>-biotin-streptavidin-enzyme bioconjugates.<sup>46</sup>

A novel amperometric immunosensor built on a glassy carbon electrode modified with a silver-MWCNT (Ag-MWCNT) composite (Figure 4d) was developed to detect  $\alpha$ -1-fetoprotein, an oncofetal glycoprotein biomarker found in several malignant diseases.<sup>65</sup> A chitosan–MnO<sub>2</sub> protective film was added on top of the Ag-MWCNT composite to prevent leaking of the composite from the electrode surface, and then gold nanoparticles were electrodeposited on the electrode to immobilize anti- $\alpha$ -1-fetoprotein. This immunosensing setup was able to quantitate  $\alpha$ -1-fetoprotein with a detection limit of 0.08 ng mL<sup>-1</sup>. Gao *et al.* developed an immunosensor for CEA using layer-by-layer assembly of positively charged carbon nanotubes wrapped by PDDA and negatively charged poly(sodium-*p*-styrene sulfonate).<sup>66</sup> Gold nanoclusters were then electrodeposited on the layered sensor surface, resulting in a high surface area and a biocompatible environment for the immobilization of capture antibodies. The immunosensor assembly could detect down to 60 pg mL<sup>-1</sup> of CEA using cyclic voltammetry (CV).

Another approach employing composite membranes of phenoxazine dye Azure I as a redox mediator and MWCNT with AuNP adsorbed on the sensor surface further improved the sensitivity of the system, yielding a detection limit of 40 pg mL<sup>-1</sup> CEA.<sup>68</sup> Finally, carbon nanotube array-based label-free electrochemical detection systems are also being developed in which the nanotube electrode tips are modified for

biorecognition. Okuno *et al.* fabricated a label-free immunosensor using microelectrode arrays modified with SWCNT (Figure 4e) for the detection of total PSA (T-PSA) by differential pulse voltammetry.<sup>67</sup> The current signals from the oxidation of tyrosine and tryptophan in the T-PSA bound to the antibodies immobilized on the SWNT sensors gave a DL of 0.25 ng mL<sup>-1</sup> for T-PSA.

**Electrochemiluminescence-Based Immunoassays.** Electrochemiluminescence (ECL) is a process in which light emission is initiated by a redox reaction occurring at an electrode surface, and its use in analytical applications has grown significantly in recent years. Several excellent reviews have reported on the mechanism, advantages, and applications of this highly sensitive and selective analytical method.<sup>69–71</sup> Advantages include use of the applied potential for precise control of reaction kinetics, compatibility with solution-phase and thin film formats, and the specificity arising from the dual requirement of a chemical label and physical localization on an electrode for signal generation. Protein measurement using ECL is typically done using particle-based immunoassays in which the ECL labels are tagged to nanoparticle bioconjugates, such as silica nanoparticles or magnetic beads, which are immobilized on the sensor surface, and the ECL signal, which is proportional to protein concentration, is measured by a charge-coupled device (CCD) or a photomultiplier tube (PMT). The most frequently used ECL label is tris(2,2'-bipyridyl)ruthenium(II), ([Ru(bpy)<sub>3</sub>]<sup>2+</sup>), which emits light when its oxidized form reacts with a suitable reductant.<sup>72</sup> Even though a number of small molecules, ions,<sup>73,74</sup> or enzymes<sup>75–77</sup> can be used as co-reactants, tripropylamine (TPrA) provides the highest sensitivity and so is the most commonly used reductant for [Ru(bpy)<sub>3</sub>]<sup>2+</sup> labels.<sup>70,71</sup> The ECL process in this system is initiated by oxidation of the sacrificial reductant TPrA at 0.9 V (using a saturated calomel electrode (SCE) reference), and the resulting products then react in a complex pathway with [Ru(bpy)<sub>3</sub>]<sup>2+</sup> to yield [Ru(bpy)<sub>3</sub>]<sup>2+\*</sup> (Scheme 2). The [Ru(bpy)<sub>3</sub>]<sup>2+</sup>/TPrA system has been used to detect cancer biomarkers, such as cancer antigen 125,<sup>78</sup> adrenocorticotrophic hormone,<sup>79</sup> PSA,<sup>80</sup> P53 protein,<sup>81</sup>  $\alpha$ -fetoprotein (AFP),<sup>82</sup> C-reactive protein,<sup>83,84</sup> and others. ECL using 100 nm [Ru(bpy)<sub>3</sub>]<sup>2+</sup>-silica nanoparticle labels has been used for the detection of PSA in



**Scheme 2. Pathway for ECL generation in the Ru(bpy)<sub>3</sub>]<sup>2+</sup>/TPrA system. The ECL pathway involves generation of ECL by reduction of [Ru(bpy)<sub>3</sub>]<sup>2+</sup> to [Ru(bpy)<sub>3</sub>]<sup>2+\*</sup> mediated by direct oxidation of TPrA on the sensor surface.**



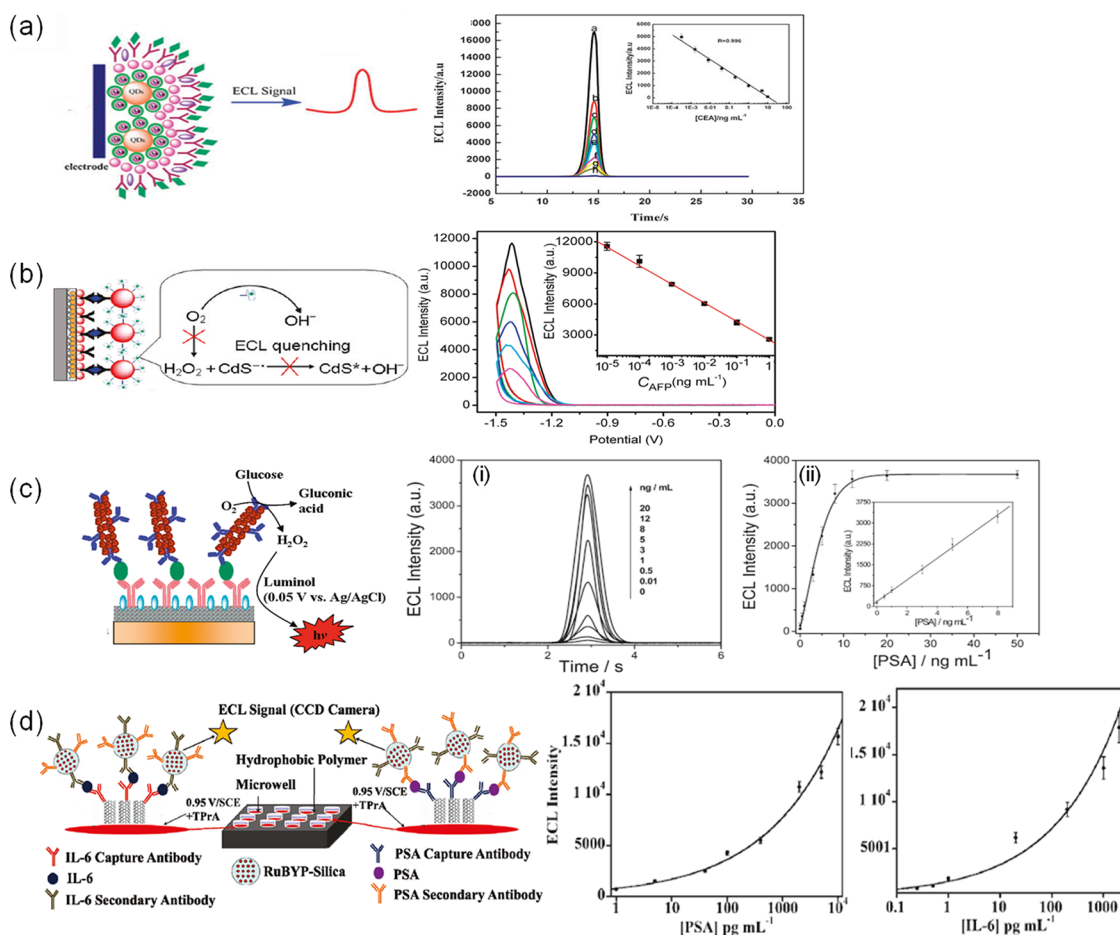


**Figure 5.** Different approaches for ECL immunosensors, with corresponding data and calibration curves. (a) ECL immunosensor employing Au-silica-CdSe-CdS QD nanostructure for the detection of CEA. Immunoassay developed on the sensor surface inhibits electron transfer and decreases ECL intensity. Adapted with permission from ref 88. Copyright 2010 RSC Publishing. (b) ECL system employing quenching of ECL upon immunocomplex formation. Adapted from ref 77. Copyright 2011 American Chemical Society. (c) ECL immunosensor assembly employing GOx label as a co-reactant to generate ECL. Adapted from ref 76. Copyright 2011 American Chemical Society. (d) ECL immunosensor developed on SWCNT-modified pyrolytic graphite electrodes using silica-Ru(bpy)<sub>3</sub><sup>2+</sup> particles. Adapted from ref 86. Copyright 2011 American Chemical Society.

the serum of cancer patients by employing single-walled carbon nanotube forest immunosensors.<sup>85</sup> Bead-based ECL immunoassays have been commercialized (e.g., Mesoscale Discovery), with typical DLs of 1–10 pg mL<sup>-1</sup> for most of the protein kits. However, commercial assay kits and instruments are relatively expensive. Current research efforts are focused on higher sensitivity and faster measurements using small sample volumes at low cost.

Rusling's group recently reported an SWCNT microwell array for highly sensitive two analyte ECL detection on a 1 × 1 in. pyrolytic graphite chip (Figure 5d).<sup>86</sup> The ECL array featured 10 μL bottomless wells, patterned in a hydrophobic polymer. SWCNT forests are fabricated on the graphite chip surface in the wells and attached with antibodies for capture of analyte proteins. Silica nanoparticles containing [Ru(bpy)<sub>3</sub>]<sup>2+</sup> and antibodies (RuBYP-silica-Ab<sub>2</sub>) were added to bind to the captured proteins, and the emitted light was measured with a CCD camera. The confinement of the

analytical spots by hydrophobic wall barriers enabled simultaneous measurement of PSA and IL-6, with a DL of 1 pg mL<sup>-1</sup> for PSA and 0.25 pg mL<sup>-1</sup> for IL-6, and showed excellent correlation with single-protein ELISAs.

Walt's group reported an optical fiber array employing polystyrene beads to detect multiple antigens simultaneously using ECL.<sup>87</sup> In this approach, antibody-coated beads were combined with a sample containing the analyte of interest and then biotinylated detection antibody, which later captured streptavidin conjugated to [Ru(bpy)<sub>3</sub>]<sup>2+</sup>. The resulting complexes were then collected into microwells of an electrode prepared from etched fiber optic bundles coated with gold. The presence of analyte was determined by collecting the ECL from the array with an EM-CCD camera connected to a microscope. The group demonstrated the method using VEGF, IL-8, and TIMP-1 as model proteins. The amplification of an ECL signal using various nanoparticles has also been demonstrated.<sup>23,88</sup>

A recent study demonstrated an ECL-based immunoassay that employed CdTe Qdots as ECL labels and dithiopersulfate as the co-reactant. Using this system with ultrathin, nanoporous gold leaf electrodes, a detection limit of  $10 \text{ pg mL}^{-1}$  for CEA was achieved.<sup>73</sup> Jie *et al.* reported a highly sensitive immunosensor for CEA, using a hybrid Au-silica-CdSe-CdS QD nanostructure that enhanced ECL intensity by 17-fold compared to pure QDs.<sup>88</sup> The hybrid structure had a core of CdSe-CdS QDs covered with a dense monolayer of AuNPs, which, in turn, were coated in silica shells (Figure 5a). The ECL intensity decreased with increasing CEA concentration, giving a DL of  $64 \text{ fg mL}^{-1}$  for CEA. The decrease in ECL intensity was attributed to increased steric hindrance of the transfer of electrons and  $\text{K}_2\text{S}_2\text{O}_8$  after formation of the immunocomplex. Another high sensitivity ECL immunosensor using quantum dots was reported by Lin *et al.*, who employed LBL modification of CNT and CdS quantum dots on a glassy carbon electrode for the detection of AFP.<sup>77</sup> After the sensor surface was modified with AuNP and capture antibodies, an immunocomplex was formed with bio-bar-coded (G-quadruplex DNA + hemin) AuNP conjugated with  $\text{Ab}_2$  (Figure 5b). The researchers attributed the resulting decrease in the QD ECL intensity primarily to the consumption of ECL coreactant ( $\text{O}_2$ ) by the bio-bar-code, which electrocatalyzes reduction of dissolved  $\text{O}_2$ . This yielded a DL of  $1 \text{ fg mL}^{-1}$  for AFP. Another study used an ECL detection system based on luminol in the presence of glucose, and  $\text{O}_2$  yielded a detection limit of  $8 \text{ pg mL}^{-1}$  for PSA (Figure 5c). In that study, Xu *et al.* used a graphene-composite-modified electrode coated with primary antibody and gold nanorods multilabeled with glucose oxidase (GOx). The gold nanorods acted as carriers of enzymes and  $\text{Ab}_2$  but also catalyzed the ECL reaction of luminol, amplifying the signal and enabling the low DL.

**Microfluidic Immunoassays and Arrays.** Microfluidics-based immunoassays offer various advantages over conventional methods because they require smaller quantities (often only nanoliters) of reagents and samples, can speed up antibody–antigen interaction (due to high surface-area-to-volume ratios and smaller length scales), and are adaptable to automated fluid handling (which can improve reproducibility and throughput). Moreover, the basic materials used to fabricate microfluidic devices can be inexpensive. These advantages make microfluidic devices promising tools for POC assays of clinical biomarkers. The goals of microfluidics research for these applications are to create sensitive, integrated, portable, clinical diagnostic tools that can detect multiple biomarkers in minimal time and with minimal sample and reagent requirements. Heineman's group was among the first to integrate microfluidics with electrochemical detection of proteins.<sup>30,89,90</sup> These systems used sandwich immunoassays in which alkaline phosphatase enzyme

labels produce electroactive products that are transported by a fluidic system to an electrode for detection. In one study, his team developed a magnetic-bead-based immunoassay in a glass microfluidic system that incorporated surface-mounted electrochemical sensors. Magnetic beads coated with sheep anti-mouse IgG were first captured on the sensor surface by applying a magnetic field, after which the antigen, secondary antibody labeled with AP, and finally the enzyme substrate *p*-aminophenyl phosphatase (PAPP) were injected sequentially. A detection limit  $50 \text{ ng mL}^{-1}$  of IgG was achieved with a measurement time of less than 20 min.

Ko and co-workers fabricated a microfluidic device by sealing a poly(dimethyl siloxane) (PDMS) top substrate, patterned with fluidic channels onto a poly(methyl methacrylate) (PMMA) bottom substrate, patterned with gold electrodes. The device was used for electrochemical biosensing of two model analytes: antiferritin antibodies and streptavidin.<sup>91</sup>

The electrode surface was modified with ferritin and biotin prior to the device assembly. After the sample was loaded into the detection chamber and an electric potential applied, a catalytic reaction of HRP labels on the streptavidin antibodies with 4-chloro-1-naphthol formed a precipitate on the sensing electrode, decreasing the effective surface area and leading to a measurable electrochemical signal.

Tang *et al.* developed a microfluidic magnetic-bead-based immunoassay for multiplexed detection of four tumor markers, AFP, CEA, cancer antigen 125, and cancer antigen 15-3 (CA 15-3), in which switching and control of electrochemical signals was achieved with an external magnet.<sup>95</sup> A detection limit of  $<0.5 \text{ } \mu\text{g mL}^{-1}$  was achieved for most of the analytes by measuring the shift in potential associated with antigen–antibody interaction. A highly sensitive 16 sensor electrochemical chip was reported by Wei *et al.*, in which individual sensors were coated with a DNA dendrimer/conducting polymer (polypyrrole) film and capture antibodies.<sup>96</sup> Oral cancer protein biomarkers IL-8 and IL-1 $\beta$  and an RNA marker, IL-8 mRNA, were measured in buffer with a DL of  $100\text{--}200 \text{ fg mL}^{-1}$  for the proteins and  $10 \text{ aM}$  for IL-8 mRNA. Somewhat higher DLs of  $3.9 \text{ fM}$  for IL-8 mRNA and  $7 \text{ pg mL}^{-1}$  for IL-8 were obtained when the system was used with human saliva samples, but even with these higher limits, oral cancer detection with 90% sensitivity and specificity was achieved.<sup>97</sup>

Recently, an integrated microfluidic device featuring a detection zone (incorporating the electrode arrays) and a separate fluid storage section was used successfully for the amperometric detection of biomarkers CEA, CA 15-3, and PSA in buffer.<sup>98</sup> The gold electrodes in the detection zone were functionalized with monolayers of carboxylic-acid-terminated dithiol and then coupled to monoclonal capture antibodies.

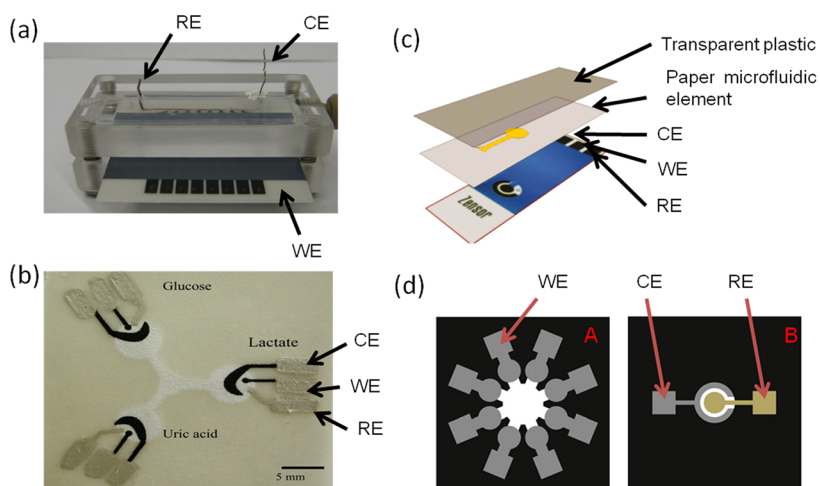


**Figure 6.** Microfluidic devices employed for electrochemical detection. (a) Microfluidic device fabricated with PMMA and an 8-electrode array for simultaneous detection of biomarkers, employing offline capture of protein analytes. Unpublished photo by B.V. Chikkaveeraiah. (b) Paper-based microfluidic device for electrochemical detection. Adapted from ref 92. Copyright 2009 American Chemical Society. (c) Paper-based device for ECL sensor. Adapted from ref 93. Copyright 2011 American Chemical Society. (d) Three-dimensional paper-based ECL device with screen printed carbon working electrodes. The common Ag/AgCl reference and carbon counter electrodes are on another paper, and interface by stacking. Adapted with permission from ref 94. Copyright 2012 Elsevier. RE, reference electrode; CE, counter electrode; WE, working electrode.

In-house prepared HRP–antibody conjugate was used to develop the electrochemical signal. Detection limits of  $0.2 \text{ ng mL}^{-1}$  for CEA,  $5.2 \text{ U mL}^{-1}$  for CA 15-3, and  $2 \text{ ng mL}^{-1}$  for PSA were obtained. The device was tested for the detection of CEA in patient serum samples, without off-chip sample preparation, and demonstrated a good correlation with ELISA. Rusling's research group recently reported a nanoparticle-based 8-electrode biosensor array coupled with a simple microfluidic system (Figure 6a).<sup>99</sup> This microfluidic immunoassay system featured a AuNP-modified screen-printed carbon array inserted into a molded PDMS channel, enclosed in a PMMA substrate and equipped with a pump and injector valve. Magnetic beads, linked to secondary antibodies and to an estimated 200 000 HRP labels per bead, were used for off-line protein capture from the serum samples. After capture of the protein analytes, the beads were washed, separated, and injected into the microfluidic device, where they were captured by antibodies on the sensor chip. An amperometric signal corresponding to analyte concentration was developed by injecting  $\text{H}_2\text{O}_2$  to activate the HRP. Multiplexed detection of PSA and IL-6 was achieved at subpicogram per milliliter DLs with assay times of approximately 1 h, including the off-line magnetic bead capture. The same group also reported low-cost gold sensor arrays made by patterning gold compact discs (CDs) to form microwells with integrated sensor electrodes, and then used these arrays in a microfluidic device to detect IL-6 in diluted serum.<sup>100</sup> The sensors were functionalized with capture antibodies, and the detection antibodies were attached *via* a biotin-streptavidin linkage to polymerized HRP (polyHRP) for signal amplification. This approach achieved an excellent sensitivity with a DL of

$10 \text{ fg mL}^{-1}$  ( $385 \text{ aM}$ ) for IL-6 in diluted serum without off-line capture or preconcentration.

**Paper-Based Microfluidic Sensors.** Recently, paper-based microfluidic devices are gaining interest as alternatives to more expensive glass and polymer-based devices for point of care analysis. Paper-based sensors have not yet been applied extensively to cancer protein biomarker detection, but there has been some promising immunosensor development. In paper-based devices, the areas of paper covered by photoresist or wax act as hydrophobic walls, confining fluid to the interior hydrophilic regions. Fluid flow is driven by the open areas of paper filling through capillary action, making these devices especially attractive for power-free applications.<sup>101</sup> Dungchai *et al.* reported the first electrochemical paper-based microfluidic device (Figure 6b) and successfully measured glucose, lactate, and uric acid in serum samples with good correlation to traditional tests.<sup>92</sup> Microfluidic channels were defined on filter paper using photolithography, and electrodes were fabricated using screen printing. Whitesides's research group, which pioneered the development of microfluidic devices, has demonstrated paper-based microfluidic immunosensors employing optical<sup>101–103</sup> and, more recently, electrochemical<sup>104</sup> detection. That group's electrochemical micro-paper-based analytical devices ( $E_{\mu}$ PADs)<sup>104</sup> are used in conjunction with a commercial hand-held glucometer for quantitative analysis of glucose, cholesterol, and lactate in human plasma and for ethanol in aqueous solution (Figure 6c).  $E_{\mu}$ PADs contain microfluidic channels, graphite electrodes, and silver electrical contacts fabricated onto chromatography paper using a combination of wax printing, annealing, and screen printing. The reagents needed for the assays are

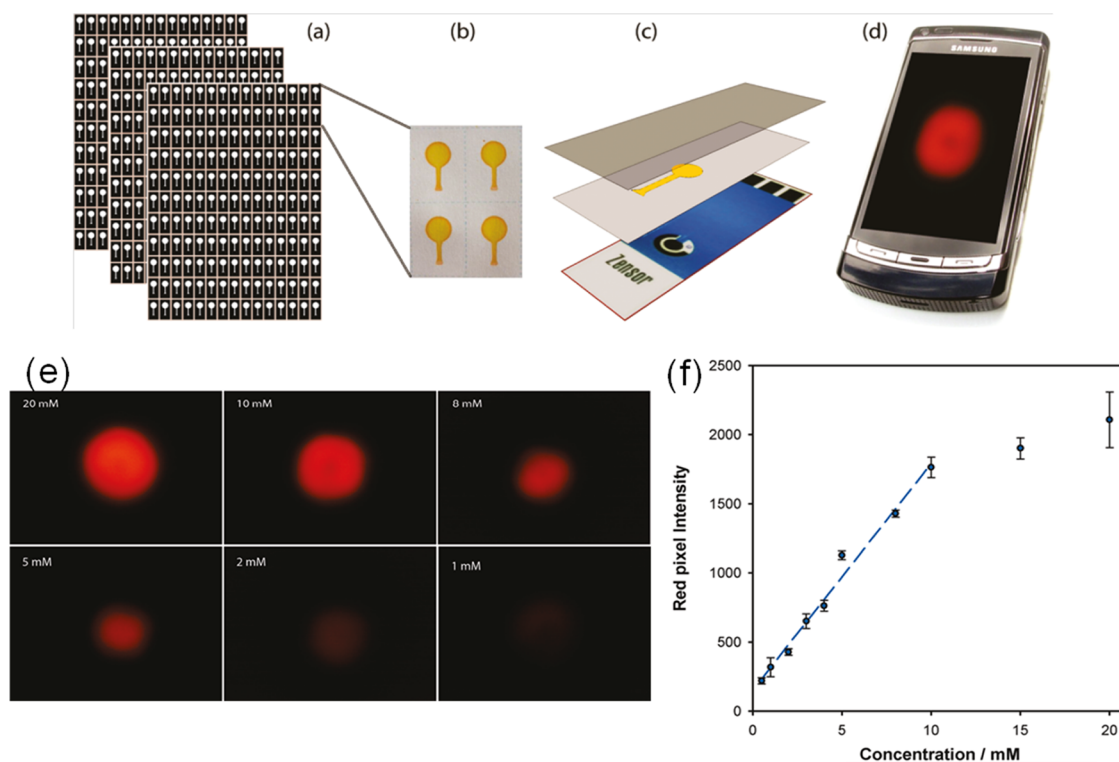


Figure 7. Paper-based microfluidic ECL sensor system. (a) Paper microfluidics produced in bulk using an inkjet printer. (b) Hydrophilic portion of the paper is filled with a 10 mM  $\text{Ru}(\text{bpy})_3^{2+}$  solution and then dried. (c) Paper substrate is then laminated onto the screen-printed electrode using transparent plastic. A drop of sample is introduced through a small aperture in the plastic at the base of the channel. Then, after the detection zone is fully wetted, a potential of 1.25 V is applied, and the sensor is placed close to the lens of a camera phone (d) to capture the resulting emission. (e) ECL images from the paper-based sensor for various concentration of DBAE. (f) Calibration curve showing ECL response between 0.5 and 20 mM DBAE, using paper microfluidic ECL sensor. Adapted from ref 93. Copyright 2011 American Chemical Society.

preloaded into the detection zone of the  $E_{\mu}$ PADs and stored dry. For analysis, a dry  $E_{\mu}$ PAD is inserted into the glucometer, and a drop of the sample is added to the exposed end of the  $E_{\mu}$ PAD. After the analyte solution is allowed to wick to the sensing region, the electrochemical readout, arising from an enzyme-catalyzed reaction using ferrocyanide as an electron-transfer mediator, is displayed on an LCD screen. The  $E_{\mu}$ PADs show good correlation with commercial test strips for the analysis of glucose in human plasma. This method is promising for the development of sensors for cancer biomarkers.

Recent advances using ECL detection with paper-based microfluidic sensors<sup>93,94</sup> also show great promise for immunosensor development. Delaney *et al.* reported the first paper-based ECL microfluidic device, for which they used inkjet printing of a hydrophobic sizing agent, alkenyl ketene dimer, to define the microfluidic channels and screen-printed electrodes (SPE).<sup>93</sup>

The device used a conventional mobile phone with a built-in camera to capture the ECL image (Figure 7). The hydrophilic portion of the paper substrate was pre-filled with  $[\text{Ru}(\text{bpy})_3]^{2+}$  solution, dried, and then fixed onto the SPE by lamination with transparent plastic. During the measurement, light emission was captured by placing the lens of the camera phone close to the sensor surface, with the pixel intensity

proportional to the amount of analytes. The sensor was used to detect two ECL co-reactants, 2-(dibutylamino)ethanol (DBAE) and a bioanalyte, nicotinamide adenine dinucleotide (NADH) with a detection limit of 0.9 and 72  $\mu\text{M}$ , respectively. Ge *et al.* recently reported a 3D paper-based ECL device in which eight carbon working electrodes (4 mm diameter) were screen printed on one piece of paper (30 mm  $\times$  30 mm) and then stacked with a second piece of paper containing screen-printed Ag/AgCl reference and carbon counter electrodes common to all eight working electrodes (Figure 6d).<sup>94</sup> Using a homemade device holder, the device was used to detect AFP, CA125, CA199, and CEA biomarkers in human serum samples with good correlation to a commercial, nonpaper ECL method. These 3D paper devices can be used to further develop simple, low-cost, disposable  $E_{\mu}$ PADs for POCs testing. The development of  $E_{\mu}$ PAD immunosensors might be particularly useful in developing countries, where scientific equipment and trained personnel may be in short supply.

## SUMMARY AND OUTLOOK

Over the past decade, in parallel with remarkable progress in nanotechnology and bioconjugation techniques, new strategies have been developed using

nanoparticles and nanostructured surfaces for electrochemical detection of cancer biomarker proteins. Low-cost, reliable, portable, multiplexed protein detection devices—especially those coupled with microfluidics—may soon enable accurate detection of panels of cancer biomarkers in blood, urine, sputum, or saliva. To ensure high reproducibility in mass production, however, bioconjugation processes must be carefully controlled; variations in the size, shape, or composition of nanomaterials, or in bioconjugation efficiency during the preparation of tags, could lead to significant variation in measurement results. New signal amplification strategies will require proper attention to the nonspecific adsorption issues that usually control detection limits in electrochemical immunoassays. Significant progress in signal amplification has been made by using multienzyme labeling on metal nanoparticles, magnetic beads, and carbon nanotubes allowing ultrasensitive detection of protein biomarkers. CNTs with their exceptionally high surface area, high sensitivity, and stability have shown promising results as platforms for multiple labels, compared to metal NPs. Advances in interfacing biomolecules with electrode surfaces and electrode surface modification with CNTs, together with these amplification strategies, have led to increasingly sensitive electrochemical immunosensors. A major challenge for electrochemical biomarker sensors is the reliable, simultaneous detection of multiple biomarkers in complex biological samples. The integration of EC and ECL immunoassays into a microfluidic format has created a strong platform for fabrication of devices for clinical diagnostics, particularly for POC. The development and deployment of these systems could ultimately lead to more rapid clinical decision making and corresponding reductions in patient stress and healthcare costs.

**Conflict of Interest:** The authors declare no competing financial interest.

**Acknowledgment.** This work was supported by the Intramural Research Program (IRP) of the National Institute of Biomedical Imaging and Bioengineering (NIBIB), National Institutes of Health (NIH), the International Cooperative Program of the National Science Foundation of China (NSFC) (81028009), and the Chinese Academy of Sciences Professorship for Senior International Scientists (2011T2J06)

## REFERENCES AND NOTES

- Atkinson, A. J.; Colburn, W. A.; DeGruttola, V. G.; DeMets, D. L.; Downing, G. J.; Hoth, D. F.; Oates, J. A.; Peck, C. C.; Schooley, R. T.; Spilker, B. A.; *et al.* Biomarkers and Surrogate Endpoints: Preferred Definitions and Conceptual Framework. *Clin. Pharmacol. Ther.* **2001**, *69*, 89–95.
- Wulfkuhle, J. D.; Liotta, L. A.; Petricoin, E. F. Proteomic Applications for the Early Detection of Cancer. *Nat. Rev. Cancer* **2003**, *3*, 267–275.
- Kulasingam, V.; Diamandis, E. P. Strategies for Discovering Novel Cancer Biomarkers through Utilization of Emerging Technologies. *Nat. Clin. Pract. Oncol.* **2008**, *5*, 588–599.
- Rusling, J. F.; Kumar, C. V.; Gutkind, J. S.; Patel, V. Measurement of Biomarker Proteins for Point-of-Care Early Detection and Monitoring of Cancer. *Analyst* **2010**, *135*, 2496–2511.
- Ludwig, J. A.; Weinstein, J. N. Biomarkers in Cancer Staging, Prognosis and Treatment Selection. *Nat. Rev. Cancer* **2005**, *5*, 845–856.
- Ferrari, M. Cancer Nanotechnology: Opportunities and Challenges. *Nat. Rev. Cancer* **2005**, *5*, 161–171.
- Kingsmore, S. F. Multiplexed Protein Measurement: Technologies and Applications of Protein and Antibody Arrays. *Nat. Rev. Drug Discovery* **2006**, *5*, 310–320.
- Polascik, T. J.; Oesterling, J. E.; Partin, A. W. Prostate Specific Antigen: A Decade of Discovery—What We Have Learned and Where We Are Going. *J. Urol.* **1999**, *162*, 293–306.
- Ghosh, A.; Heston, W. D. Tumor Target Prostate Specific Membrane Antigen (PSMA) and Its Regulation in Prostate Cancer. *J. Cell. Biochem.* **2004**, *91*, 528–539.
- Chang, S. S.; Reuter, V. E.; Heston, W. D.; Bander, N. H.; Grauer, L. S.; Gaudin, P. B. Five Different Anti-Prostate-Specific Membrane Antigen (PSMA) Antibodies Confirm PSMA Expression in Tumor-Associated Neovasculature. *Cancer Res.* **1999**, *59*, 3192–3198.
- Riedel, F.; Zaiss, I.; Herzog, D.; Gotte, K.; Naim, R.; Hormann, K. Serum Levels of Interleukin-6 in Patients with Primary Head and Neck Squamous Cell Carcinoma. *Anticancer Res.* **2005**, *25*, 2761–2765.
- Mujagic, Z.; Mujagic, H.; Prnjavorac, B. The Relationship between Circulating Carcinoembryonic Antigen (CEA) Levels and Parameters of Primary Tumor and Metastases in Breast Cancer Patients. *Med. Arh.* **2004**, *58*, 23–26.
- Findlay, J. W.; Smith, W. C.; Lee, J. W.; Nordblom, G. D.; Das, I.; DeSilva, B. S.; Khan, M. N.; Bowsher, R. R. Validation of Immunoassays for Bioanalysis: A Pharmaceutical Industry Perspective. *J. Pharm. Biomed. Anal.* **2000**, *21*, 1249–1273.
- Hawkrigde, A. M.; Muddiman, D. C. Mass Spectrometry-Based Biomarker Discovery: Toward a Global Proteome Index of Individuality. *Annu. Rev. Anal. Chem.* **2009**, *2*, 265–277.
- Hanash, S. M.; Pitteri, S. J.; Faca, V. M. Mining the Plasma Proteome for Cancer Biomarkers. *Nature* **2008**, *452*, 571–579.
- Wilson, D. S.; Nock, S. Recent Developments in Protein Microarray Technology. *Angew. Chem., Int. Ed.* **2003**, *42*, 494–500.
- Lee, H. J.; Wark, A. W.; Corn, R. M. Microarray Methods for Protein Biomarker Detection. *Analyst* **2008**, *133*, 975–983.
- Bensmail, H.; Haoudi, A. Postgenomics: Proteomics and Bioinformatics in Cancer Research. *J. Biomed. Biotechnol.* **2003**, *2003*, 217–230.
- Rasooly, A.; Jacobson, J. Development of Biosensors for Cancer Clinical Testing. *Biosens. Bioelectron.* **2006**, *21*, 1851–1858.
- Healy, D. A.; Hayes, C. J.; Leonard, P.; McKenna, L.; O'Kennedy, R. Biosensor Developments: Application to Prostate-Specific Antigen Detection. *Trends Biotechnol.* **2007**, *25*, 125–131.
- Wang, J.; Liu, G.; Jan, M. R. Ultrasensitive Electrical Biosensing of Proteins and DNA: Carbon-Nanotube Derived Amplification of the Recognition and Transduction Events. *J. Am. Chem. Soc.* **2004**, *126*, 3010–3011.
- Willner, I.; Katz, E. Magnetic Control of Electrocatalytic and Bioelectrocatalytic Processes. *Angew. Chem., Int. Ed.* **2003**, *42*, 4576–4588.
- Choi, Y. E.; Kwak, J. W.; Park, J. W. Nanotechnology for Early Cancer Detection. *Sensors* **2010**, *10*, 428–455.
- Wang, J. Nanomaterial-Based Electrochemical Biosensors. *Analyst* **2005**, *130*, 421–426.
- Wang, J.; Katz, E.; Willner, I. Biomaterial-Nanoparticle Hybrid Systems for Sensing and Electronic Devices. In *Bioelectronics: From Theory to Applications*; Katz, E., Willner, I., Eds.; Wiley-VCH: Weinheim, Germany, 2005; pp 231–264.
- Wang, J. Electrochemical Biosensors: Towards Point-of-Care Cancer Diagnostics. *Biosens. Bioelectron.* **2006**, *21*, 1887–1892.

27. Wang, J. Nanoparticle-Based Electrochemical Bioassays of Proteins. *Electroanalysis* **2007**, *19*, 769–776.
28. Zhang, H.; Meyerhoff, M. E. Gold-Coated Magnetic Particles for Solid-Phase Immunoassays: Enhancing Immobilized Antibody Binding Efficiency and Analytical Performance. *Anal. Chem.* **2006**, *78*, 609–616.
29. Tsai, H. Y.; Hsu, C. F.; Chiu, I. W.; Fuh, C. B. Detection of C-Reactive Protein Based on Immunoassay Using Antibody-Conjugated Magnetic Nanoparticles. *Anal. Chem.* **2007**, *79*, 8416–8419.
30. Choi, J. W.; Oh, K. W.; Thomas, J. H.; Heineman, W. R.; Halsall, H. B.; Nevin, J. H.; Helmicki, A. J.; Henderson, H. T.; Ahn, C. H. An Integrated Microfluidic Biochemical Detection System for Protein Analysis with Magnetic Bead-Based Sampling Capabilities. *Lab Chip* **2002**, *2*, 27–30.
31. Centi, S.; Tombelli, S.; Minunni, M.; Mascini, M. Aptamer-Based Detection of Plasma Proteins by an Electrochemical Assay Coupled to Magnetic Beads. *Anal. Chem.* **2007**, *79*, 1466–1473.
32. Thomas, J. H.; Kim, S. K.; Hesketh, P. J.; Halsall, H. B.; Heineman, W. R. Microbead-Based Electrochemical Immunoassay with Interdigitated Array Electrodes. *Anal. Biochem.* **2004**, *328*, 113–122.
33. Franzreb, M.; Siemann-Herzberg, M.; Holey, T. J.; Thomas, O. R. Protein Purification Using Magnetic Adsorbent Particles. *Appl. Microbiol. Biotechnol.* **2006**, *70*, 505–516.
34. Verpoorte, E. Beads and Chips: New Recipes for Analysis. *Lab Chip* **2003**, *3*, 60N–68N.
35. Mani, V.; Chikkaveeraiah, B. V.; Rusling, J. F. Magnetic Particles in Ultrasensitive Biomarker Protein Measurements for Cancer Detection and Monitoring. *Expert Opin. Med. Diagn.* **2011**, *5*, 381–391.
36. Xie, J.; Jon, S. Magnetic Nanoparticle-Based Theranostics. *Theranostics* **2012**, *2*, 122–124.
37. Zani, A.; Laschi, S.; Mascini, M.; Marrazza, G. A New Electrochemical Multiplexed Assay for PSA Cancer Marker Detection. *Electroanalysis* **2011**, *23*, 91–99.
38. Sarkar, P.; Ghosh, D.; Bhattacharyay, D.; Setford, S. J.; Turner, A. P. F. Electrochemical Immunoassay for Free Prostate Specific Antigen (f-PSA) Using Magnetic Beads. *Electroanalysis* **2008**, *20*, 1414–1420.
39. Wang, J.; Liu, G.; Munge, B.; Lin, L.; Zhu, Q. DNA-Based Amplified Bioelectronic Detection and Coding of Proteins. *Angew. Chem., Int. Ed.* **2004**, *43*, 2158–2161.
40. Munge, B.; Liu, G.; Collins, G.; Wang, J. Multiple Enzyme Layers on Carbon Nanotubes for Electrochemical Detection Down to 80 DNA Copies. *Anal. Chem.* **2005**, *77*, 4662–4666.
41. Katz, E.; Willner, I. Enhancement of Bioelectrocatalytic Processes by the Rotation of Mediator-Functionalized Magnetic Particles on Electrode Surfaces: Comparison with Rotating Disk Electrode. *Electroanalysis* **2005**, *17*, 1616–1626.
42. Yu, X.; Munge, B.; Patel, V.; Jensen, G.; Bhirde, A.; Gong, J. D.; Kim, S. N.; Gillespie, J.; Gutkind, J. S.; Papadimitrakopoulos, F.; et al. Carbon Nanotube Amplification Strategies for Highly Sensitive Immunodetection of Cancer Biomarkers. *J. Am. Chem. Soc.* **2006**, *128*, 11199–11205.
43. Mani, V.; Chikkaveeraiah, B. V.; Patel, V.; Gutkind, J. S.; Rusling, J. F. Ultrasensitive Immunosensor for Cancer Biomarker Proteins Using Gold Nanoparticle Film Electrodes and Multienzyme-Particle Amplification. *ACS Nano* **2009**, *3*, 585–594.
44. Munge, B. S.; Coffey, A. L.; Doucette, J. M.; Somba, B. K.; Malhotra, R.; Patel, V.; Gutkind, J. S.; Rusling, J. F. Nanostructured Immunosensor for Attomolar Detection of Cancer Biomarker Interleukin-8 Using Massively Labeled Superparamagnetic Particles. *Angew. Chem., Int. Ed.* **2011**, *50*, 7915–7918.
45. Tang, D.; Yuan, R.; Chai, Y. Ultrasensitive Electrochemical Immunosensor for Clinical Immunoassay Using Thionine-Doped Magnetic Gold Nanospheres as Labels and Horseradish Peroxidase as Enhancer. *Anal. Chem.* **2008**, *80*, 1582–1588.
46. Munge, B. S.; Krause, C. E.; Malhotra, R.; Patel, V.; Gutkind, J. S.; Rusling, J. F. Electrochemical Immunosensors for Interleukin-6. Comparison of Carbon Nanotube Forest and Gold Nanoparticle Platforms. *Electrochem. Commun.* **2009**, *11*, 1009–1012.
47. Munge, B. S.; Fisher, J.; Millord, L. N.; Krause, C. E.; Dowd, R. S.; Rusling, J. F. Sensitive Electrochemical Immunosensor for Matrix Metalloproteinase-3 Based on Single-Wall Carbon Nanotubes. *Analyst* **2010**, *135*, 1345–1350.
48. Tang, D.; Ren, J. *In Situ* Amplified Electrochemical Immunoassay for Carcinoembryonic Antigen Using Horseradish Peroxidase-Encapsulated Nanogold Hollow Microspheres as Labels. *Anal. Chem.* **2008**, *80*, 8064–8070.
49. Ambrosi, A.; Castaneda, M. T.; Killard, A. J.; Smyth, M. R.; Alegret, S.; Merkoci, A. Double-Codified Gold Nanolabels for Enhanced Immunoanalysis. *Anal. Chem.* **2007**, *79*, 5232–5240.
50. Malhotra, R.; Patel, V.; Vaque, J. P.; Gutkind, J. S.; Rusling, J. F. Ultrasensitive Electrochemical Immunosensor for Oral Cancer Biomarker IL-6 Using Carbon Nanotube Forest Electrodes and Multilabel Amplification. *Anal. Chem.* **2010**, *82*, 3118–3123.
51. Wan, Y.; Deng, W.; Su, Y.; Zhu, X.; Peng, C.; Hu, H.; Peng, H.; Song, S.; Fan, C. Carbon Nanotube-Based Ultrasensitive Multiplexing Electrochemical Immunosensor for Cancer Biomarkers. *Biosens. Bioelectron.* **2011**, *30*, 93–99.
52. Dequaire, M.; Degrand, C.; Limoges, B. An Electrochemical Metalloimmunoassay Based on a Colloidal Gold Label. *Anal. Chem.* **2000**, *72*, 5521–5528.
53. Guo, H.; He, N.; Ge, S.; Yang, D.; Zhang, J. MCM-41 Mesoporous Material Modified Carbon Paste Electrode for the Determination of Cardiac Troponin I by Anodic Stripping Voltammetry. *Talanta* **2005**, *68*, 61–66.
54. Liu, G.; Wang, J.; Kim, J.; Jan, M. R.; Collins, G. E. Electrochemical Coding for Multiplexed Immunoassays of Proteins. *Anal. Chem.* **2004**, *76*, 7126–7130.
55. Wang, J. Nanomaterial-Based Amplified Transduction of Biomolecular Interactions. *Small* **2005**, *1*, 1036–1043.
56. Daniels, J. S.; Pourmand, N. Label-Free Impedance Biosensors: Opportunities and Challenges. *Electroanalysis* **2007**, *19*, 1239–1257.
57. Park, S. J.; Taton, T. A.; Mirkin, C. A. Array-Based Electrical Detection of DNA with Nanoparticle Probes. *Science* **2002**, *295*, 1503–1506.
58. Li, J.; Xue, M.; Wang, H.; Cheng, L.; Gao, L.; Lu, Z.; Chan, M. Amplifying the Electrical Hybridization Signals of DNA Array by Multilayer Assembly of Au Nanoparticle Probes. *Analyst* **2003**, *128*, 917–923.
59. Gooding, J. J. Nanostructuring Electrodes with Carbon Nanotubes: A Review on Electrochemistry and Applications for Sensing. *Electrochim. Acta* **2005**, *50*, 3049–3060.
60. Kim, S. N.; Rusling, J. F.; Papadimitrakopoulos, F. Carbon Nanotubes for Electronic and Electrochemical Detection of Biomolecules. *Adv. Mater.* **2007**, *19*, 3214–3228.
61. Wang, J. Carbon-Nanotube Based Electrochemical Biosensors: A Review. *Electroanalysis* **2005**, *17*, 7–14.
62. Ahammad, A. J. S.; Lee, J. J.; Rahman, M. A. Electrochemical Sensors Based on Carbon Nanotubes. *Sensors* **2009**, *8*, 2289–2319.
63. Chikkaveeraiah, B. V.; Bhirde, A.; Malhotra, R.; Patel, V.; Gutkind, J. S.; Rusling, J. F. Single-Wall Carbon Nanotube Forest Arrays for Immunochemical Measurement of Four Protein Biomarkers for Prostate Cancer. *Anal. Chem.* **2009**, *81*, 9129–9134.
64. Malhotra, R.; Papadimitrakopoulos, F.; Rusling, J. F. Sequential Layer Analysis of Protein Immunosensors Based on Single Wall Carbon Nanotube Forests. *Langmuir* **2010**, *26*, 15050–15056.
65. Che, X.; Yuan, R.; Chai, Y.; Li, J.; Song, Z.; Wang, J. Amperometric Immunosensor for the Determination of Alpha-1-Fetoprotein Based on Multiwalled Carbon Nanotube-Silver Nanoparticle Composite. *J. Colloid Interface Sci.* **2010**, *345*, 174–180.

66. Gao, X.; Zhang, Y.; Chen, H.; Chen, Z.; Lin, X. Amperometric Immunosensor for Carcinoembryonic Antigen Detection with Carbon Nanotube-Based Film Decorated with Gold Nanoclusters. *Anal. Biochem.* **2011**, *414*, 70–76.
67. Okuno, J.; Maehashi, K.; Kerman, K.; Takamura, Y.; Matsumoto, K.; Tamiya, E. Label-Free Immunosensor for Prostate-Specific Antigen Based on Single-Walled Carbon Nanotube Array-Modified Microelectrodes. *Biosens. Bioelectron.* **2007**, *22*, 2377–2381.
68. Li, N.; Yuan, R.; Chai, Y.; Chen, S.; An, H.; Li, W. New Antibody Immobilization Strategy Based on Gold Nanoparticles and Azure I/Multi-Walled Carbon Nanotube Composite Membranes for an Amperometric Enzyme Immunosensor. *J. Phys. Chem. C* **2007**, *111*, 8443–8450.
69. Richter, M. M. Electrochemiluminescence (ECL). *Chem. Rev.* **2004**, *104*, 3003–3036.
70. Forster, R. J.; Bertonecello, P.; Keyes, T. E. Electrogenated Chemiluminescence. *Annu. Rev. Anal. Chem.* **2009**, *2*, 359–385.
71. Miao, W. Electrogenated Chemiluminescence and Its Biorelated Applications. *Chem. Rev.* **2008**, *108*, 2506–2553.
72. Debad, J. B.; Glezer, E. N.; Leland, J. K.; Sigal, G. B.; Wholstadtter, J. Clinical and Biological Applications of ECL. In *Electrogenated Chemiluminescence*; Bard, A. J., Ed.; Marcel Dekker: New York, 2004; pp 359–396.
73. Li, X.; Wang, R.; Zhang, X. Electrochemiluminescence Immunoassay at a Nanoporous Gold Leaf Electrode and Using CdTe Quantum Dots as Labels. *Microchim. Acta* **2011**, *172*, 285–290.
74. Li, C.; Lin, J.; Guo, Y.; Zhang, S. A Novel Electrochemiluminescent Reagent of Cyclometalated Iridium Complex-Based DNA Biosensor and Its Application in Cancer Cell Detection. *Chem. Commun.* **2011**, *47*, 4442–4444.
75. Kurita, R.; Arai, K.; Nakamoto, K.; Kato, D.; Niwa, O. Development of Electrogenated Chemiluminescence-Based Enzyme Linked Immunosorbent Assay for Sub-pM Detection. *Anal. Chem.* **2010**, *82*, 1692–1697.
76. Xu, S.; Liu, Y.; Wang, T.; Li, J. Positive Potential Operation of a Cathodic Electrogenated Chemiluminescence Immunosensor Based on Luminol and Graphene for Cancer Biomarker Detection. *Anal. Chem.* **2011**, *83*, 3817–3823.
77. Lin, D.; Wu, J.; Yan, F.; Deng, S.; Ju, H. Ultrasensitive Immunoassay of Protein Biomarker Based on Electrochemiluminescent Quenching of Quantum Dots by Hemin Bio-Bar-Coded Nanoparticle Tags. *Anal. Chem.* **2011**, *83*, 5214–5221.
78. van Ingen, H. E.; Chan, D. W.; Hubl, W.; Miyachi, H.; Molina, R.; Pitzel, L.; Ruibal, A.; Rymer, J. C.; Domke, I. Analytical and Clinical Evaluation of an Electrochemiluminescence Immunoassay for the Determination of CA 125. *Clin. Chem.* **1998**, *44*, 2530–2536.
79. Verschraegen, I.; Anckaert, E.; Schiettecatte, J.; Mees, M.; Garrido, A.; Hermsen, D.; Lentjes, E. G.; Liebert, A.; Roth, H. J.; Stamminger, G.; et al. Multicenter Evaluation of a Rapid Electrochemiluminescent Adrenocorticotrophic Hormone (ACTH) Immunoassay. *Clin. Chim. Acta* **2007**, *380*, 75–80.
80. Xu, X. H.; Jeffers, R. B.; Gao, J.; Logan, B. Novel Solution-Phase Immunoassays for Molecular Analysis of Tumor Markers. *Analyst* **2001**, *126*, 1285–1292.
81. Yan, G.; Xing, D.; Tan, S.; Chen, Q. Rapid and Sensitive Immunomagnetic-Electrochemiluminescent Detection of P53 Antibodies in Human Serum. *J. Immunol. Methods* **2004**, *288*, 47–54.
82. Namba, Y.; Usami, M.; Suzuki, O. Highly Sensitive Electrochemiluminescence Immunoassay Using the Ruthenium Chelate-Labeled Antibody Bound to the Magnetic Micro Beads. *Anal. Sci.* **1999**, *15*, 1087–1093.
83. Miao, W.; Bard, A. J. Electrogenated Chemiluminescence. 80. C-Reactive Protein Determination at High Amplification with [Ru(Bpy)<sub>3</sub>]<sup>2+</sup>-Containing Microspheres. *Anal. Chem.* **2004**, *76*, 7109–7113.
84. Zhan, W.; Bard, A. J. Electrogenated Chemiluminescence. 83. Immunoassay of Human C-Reactive Protein by Using [Ru(Bpy)<sub>3</sub>]<sup>2+</sup>-Encapsulated Liposomes as Labels. *Anal. Chem.* **2007**, *79*, 459–463.
85. Sardesai, N.; Pan, S.; Rusling, J. Electrochemiluminescent Immunosensor for Detection of Protein Cancer Biomarkers Using Carbon Nanotube Forests and [Ru(Bpy)<sub>3</sub>]<sup>2+</sup>-Doped Silica Nanoparticles. *Chem. Commun.* **2009**, 4968–4970.
86. Sardesai, N. P.; Barron, J. C.; Rusling, J. F. Carbon Nanotube Microwell Array for Sensitive Electrochemiluminescent Detection of Cancer Biomarker Proteins. *Anal. Chem.* **2011**, *83*, 6698–6703.
87. Deiss, F.; LaFratta, C. N.; Symer, M.; Blicharz, T. M.; Sojic, N.; Walt, D. R. Multiplexed Sandwich Immunoassays Using Electrochemiluminescence Imaging Resolved at the Single Bead Level. *J. Am. Chem. Soc.* **2009**, *131*, 6088–6089.
88. Jie, G. F.; Liu, P.; Zhang, S. S. Highly Enhanced Electrochemiluminescence of Novel Gold/Silica/CdSe-CdS Nanostructures for Ultrasensitive Immunoassay of Protein Tumor Marker. *Chem. Commun.* **2010**, *46*, 1323–1325.
89. Ronkainen-Matsuno, N. J.; Thomas, J. H.; Halshall, H. B.; Heineman, W. R. Electrochemical Immunoassay Moving into the Fast Lane. *Trends Anal. Chem.* **2002**, *21*, 213–225.
90. Bange, A.; Halsall, H. B.; Heineman, W. R. Microfluidic Immunosensor Systems. *Biosens. Bioelectron.* **2005**, *20*, 2488–2503.
91. Soo, Ko, J.; Yoon, H. C.; Yang, H.; Pyo, H. B.; Hyo Chung, K.; Jin Kim, S.; Tae Kim, Y. A Polymer-Based Microfluidic Device for Immunosensing Biochips. *Lab Chip* **2003**, *3*, 106–113.
92. Dungchai, W.; Chailapakul, O.; Henry, C. S. Electrochemical Detection for Paper-Based Microfluidics. *Anal. Chem.* **2009**, *81*, 5821–5826.
93. Delaney, J. L.; Hogan, C. F.; Tian, J.; Shen, W. Electrogenated Chemiluminescence Detection in Paper-Based Microfluidic Sensors. *Anal. Chem.* **2011**, *83*, 1300–1306.
94. Ge, L.; Yan, J.; Song, X.; Yan, M.; Ge, S.; Yu, J. Three-Dimensional Paper-Based Electrochemiluminescence Immunoassay for Multiplexed Measurement of Biomarkers and Point-of-Care Testing. *Biomaterials* **2012**, *33*, 1024–1031.
95. Tang, D.; Yuan, R.; Chai, Y. Magnetic Control of an Electrochemical Microfluidic Device with an Arrayed Immunosensor for Simultaneous Multiple Immunoassays. *Clin. Chem.* **2007**, *53*, 1323–1329.
96. Wei, F.; Liao, W.; Xu, Z.; Yang, Y.; Wong, D. T.; Ho, C. M. Bio/Abiotic Interface Constructed from Nanoscale DNA Dendrimer and Conducting Polymer for Ultrasensitive Biomolecular Diagnosis. *Small* **2009**, *5*, 1784–1790.
97. Wei, F.; Patel, P.; Liao, W.; Chaudhry, K.; Zhang, L.; Arellano-Garcia, M.; Hu, S.; Elashoff, D.; Zhou, H.; Shukla, S.; et al. Electrochemical Sensor for Multiplex Biomarkers Detection. *Clin. Cancer Res.* **2009**, *15*, 4446–4452.
98. Fragoso, A.; Latta, D.; Laboria, N.; von Gernar, F.; Hansen-Hagge, T. E.; Kemmner, W.; Gartner, C.; Klemm, R.; Drese, K. S.; O'Sullivan, C. K. Integrated Microfluidic Platform for the Electrochemical Detection of Breast Cancer Markers in Patient Serum Samples. *Lab Chip* **2011**, *11*, 625–631.
99. Chikkaveeraiiah, B. V.; Mani, V.; Patel, V.; Gutkind, J. S.; Rusling, J. F. Microfluidic Electrochemical Immunoarray for Ultrasensitive Detection of Two Cancer Biomarker Proteins in Serum. *Biosens. Bioelectron.* **2011**, *26*, 4477–4483.
100. Tang, C. K.; Vaze, A.; Rusling, J. F. Fabrication of Immunosensor Microwell Arrays from Gold Compact Discs for Detection of Cancer Biomarker Proteins. *Lab Chip* **2012**, *12*, 281–286.
101. Martinez, A. W.; Phillips, S. T.; Whitesides, G. M. Three-Dimensional Microfluidic Devices Fabricated in Layered Paper and Tape. *Proc. Natl. Acad. Sci. U.S.A.* **2008**, *105*, 19606–19611.
102. Martinez, A. W.; Phillips, S. T.; Carrillo, E.; Thomas, S. W., III; Sindi, H.; Whitesides, G. M. Simple Telemedicine for Developing Regions: Camera Phones and Paper-Based Microfluidic Devices for Real-Time, Off-Site Diagnosis. *Anal. Chem.* **2008**, *80*, 3699–3707.

103. Ellerbee, A. K.; Phillips, S. T.; Siegel, A. C.; Mirica, K. A.; Martinez, A. W.; Striehl, P.; Jain, N.; Prentiss, M.; Whitesides, G. M. Quantifying Colorimetric Assays in Paper-Based Microfluidic Devices by Measuring the Transmission of Light through Paper. *Anal. Chem.* **2009**, *81*, 8447–8452.
104. Nie, Z.; Nijhuis, C. A.; Gong, J.; Chen, X.; Kumachev, A.; Martinez, A. W.; Narovlyansky, M.; Whitesides, G. M. Electrochemical Sensing in Paper-Based Microfluidic Devices. *Lab Chip* **2010**, *10*, 477–483.